Computational Sciences and Engineering 5(1) (2025) 187-209

University of Guilan

Computational Sciences and Engineering

journal homepage: https://cse.guilan.ac.ir/

Numerical Investigation of Ricochet Behavior of APM2 Armor-Piercing Projectiles on Metallic Targets by Considering Rotational Effects

Pooya Pirali[a,*], Mohsen Heydari Beni[a], Sajjad Nourbakhsh Shabanlou[a], Jafar Eskandari Jam[a], Majid Eskandari Shahraki[b]

[a] Faculty of Materials and Manufacturing Technologies, Malek Ashtar University of Technology, Tehran, Iran.
[b] Department of Aerospace Engineering, Faculty of Engineering, Ferdowsi University of Mashhad, Mashhad, Iran

ARTICLE INFO

Article history:
Received 3 October 2025
Received in revised form 20 November 2025
Accepted 22 November 2025
Available online 22 November 2025

Keywords:
APM2 armor-piercing projectile
Oblique impact
Penetration
Critical ricochet angle
Axial rotation
LS-DYNA

ABSTRACT

In real-world scenarios, projectile impacts on targets rarely occur at perfectly normal angles. This study employs the finite element software LS-DYNA to numerically investigate the oblique penetration and ricochet behavior of the 7.62 mm APM2 armor-piercing projectile against AA6082-T4 aluminum alloy targets. The material behavior was modeled using the modified Johnson-Cook constitutive model, with failure assessed via the Cockcroft-Latham criterion. The model was validated against experimental data, showing good agreement with exit velocities. A central focus was to evaluate the common simplification of neglecting projectile rotation. Parametric analyses revealed that the critical ricochet angle (θc) increases with impact velocity, rising from 62° at 830 m/s to 80° at 1800 m/s for a 20 mm target. Crucially, while axial rotation was found to have a negligible effect on θc (variation < 1°), it significantly reduced the projectile's residual velocity by 5–15% and influenced its trajectory. Additional analyses showed that target thickness and projectile nose shape are also dominant factors; for instance, θc decreased from 74° to 65° as thickness increased from 10 mm to 30 mm. The results demonstrate that while rotation can be ignored for estimating the critical angle, neglecting it leads to substantial inaccuracies in predicting residual velocity and energy, and is therefore not recommended for high-fidelity simulations. These findings provide critical insights for optimizing armor design and improving the accuracy of ballistic simulations.

* Corresponding author.
E-mail addresses: ppirali@mut.ac.ir (P. Pirali)

https://doi.org/10.22124/cse.2025.31861.1128

1. Introduction

Research on impact and penetration dynamics has been a major focus since the late 19th century and became particularly prominent in the 20th century within ballistic engineering, armor design, and structural protection. Understanding projectile behavior during impact with different targets is essential, as it directly contributes to the development of improved military equipment, armored vehicles, and protective structures. Early studies relied mainly on field and laboratory experiments, which were time-consuming, costly, and often restricted to controlled testing environments [1]. In recent decades, advances in computational technology have enabled the use of analytical methods and, more importantly, numerical simulations [2]. These tools have made it possible to analyze more complex conditions, such as oblique impacts and projectile rotation effects.

With the advancement of computational modeling, numerical simulations have become essential for understanding these phenomena. Badurowicz and Pacek (2022), for instance, employed a finite element model to estimate the temperature of a 5.56×45 mm SS109 projectile during oblique impact on a steel plate and successfully validated the results with experimental observations [3]. Analytical studies have also contributed to the field by developing simplified but physically meaningful models. Wu, Tao, and Xue (2022) proposed an analytical formulation to predict the ricochet range of an ogive-nosed projectile penetrating a steel target under oblique impact, demonstrating strong agreement with experimental data [4].

Material advancements have further motivated new research directions. Zhang et al. (2025) examined the ballistic performance of a tungsten fiber-reinforced metallic-glass composite under oblique impact and found that high-angle impacts reduce the asymmetric self-sharpening effect of the projectile's nose, thereby increasing the likelihood of ricochet [5]. Data-driven approaches have also emerged in ricochet analysis. For instance, Eren et al. (2024) used machine-learning techniques—specifically random forests—to classify ricochet mark morphologies produced on concrete by different ammunition types and distances [6]. Similarly, Paige and colleagues (2025) applied elliptical Fourier analysis to characterize the plan-view shape of ricochet impact marks, revealing substantial overlap among ammunition types and highlighting challenges in forensic identification [7].

From the structural engineering perspective, recent studies have analyzed the oblique impact resistance of concrete and composite targets, showing that obliquity significantly influences penetration depth, ricochet behavior, and damage patterns [8].Taken together, the literature indicates that key parameters influencing ricochet—such as projectile geometry, length-to-diameter ratio, impact angle, velocity, rotation, and target properties—are not yet fully understood in an integrated framework.

A key principle in this field is that perfectly normal impacts—those occurring at a 90-degree angle to the target—are uncommon in real operational environments. Most impacts occur at oblique angles, which increases both the mechanical and dynamic complexity of the problem [9]. The absence of axial symmetry in oblique impacts also limits the effectiveness of analytical solutions, often making experimental or numerical methods necessary.

Another influential factor is the rotation of the projectile around its longitudinal axis, typically generated by barrel rifling. This rotation enhances flight stability and improves accuracy, yet it

may also introduce unexpected effects such as trajectory deviation or altered ricochet behavior [10].

The goal of this article is to offer a comprehensive framework for understanding projectile ricochet. First, projectiles are classified based on their length-to-diameter ratio (L/D), separating them into short (L/D ≈ 1) and long (L/D > 1) categories [1]. This ratio has a direct impact on stability and penetration performance. Additionally, the geometry of the projectile nose—whether flat, conical, hemispherical, or composite—significantly affects its interaction with the target. Each nose shape generates distinct penetration and ricochet patterns [11]. This is illustrated in ***Figure 1***, which compares the penetration profiles of flat (A), hemispherical (B), and conical (C) nose projectiles.

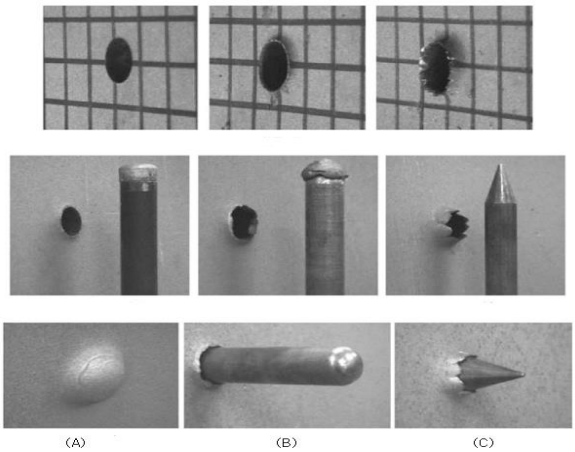

Figure 1. Details of three types of projectiles and the target affected by each. (A) Flat-nosed projectile, (B) Hemispherical-nosed projectile, and (C) Conical-nosed projectile [11].

The impact angle is another determining parameter. Impacts are generally classified into two types: perpendicular (90°) and oblique (<90°) [9]. During oblique impacts, the projectile may rotate inside the target, deviate from its trajectory, or ricochet. The occurrence of these behaviors depends on factors such as impact velocity, material properties, and the angle of obliquity. A schematic representation of the impact angle is shown in ***Figure 2***.

Several parameters—including velocity, the materials of both projectile and target, the projectile's aspect ratio, and its nose geometry—have been identified as key factors governing ricochet. These aspects have been examined extensively in previous studies [12–15].

Projectile stability is strongly influenced by its rotational motion, which is generated by the interaction with the barrel rifling and provides gyroscopic stabilization [10]. The rotational speed can be estimated using the Greenhill formula (1879):

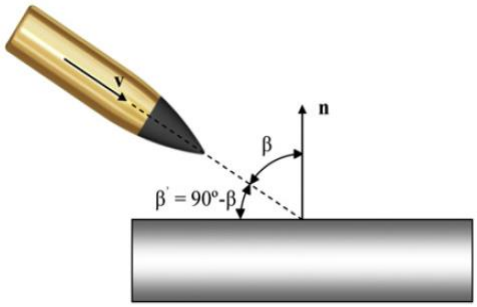

Figure 2. Projectile impact angle with the target

$$S = \frac{V_0}{Twist} \tag{1}$$

$$Twist = \frac{CD^2}{L} \times \sqrt{\frac{SG}{10.9}} \quad (in) \tag{2}$$

Here, S represents the twist rate (turns per inch), L is the projectile length, and D is its diameter (in inches) [10]. This rotational stability is essential for firing accuracy, yet its influence on ricochet behavior has been less studied. Research in this field can be grouped into three main approaches:

1. Analytical/theoretical methods [2, 12], based on mathematical models,
2. Experimental methods [13–15], providing real-world data, and
3. Numerical/simulation methods [16–21], which allow investigation of complex scenarios using advanced software such as LS-DYNA.

This study focuses on numerical simulations, with particular attention to axial rotation, aiming to fill gaps in the understanding of ricochet phenomena. Validation against experimental data, along with parametric analyses of factors such as impact velocity, target thickness, and projectile nose shape, enhances the accuracy and reliability of the models.

1.1 Research Motivation and Novelty

The ricochet behavior of spin-stabilized armor-piercing projectiles has been widely studied; however, most existing investigations either neglect projectile axial rotation or simplify its influence through symmetry assumptions. This leads to an incomplete description of post-impact dynamics, particularly for high-velocity oblique impacts where rotational torque, lateral deviation, and frictional energy loss become non-negligible. The present work addresses this gap by explicitly modeling the coupled effects of axial rotation, nose geometry, target thickness, and length-to-diameter ratio on the ricochet response of the APM2 projectile using LS-DYNA.

The novelty of this study can be summarized in four key advancements:

1. **Explicit inclusion of projectile spin in 3D simulations**
   Unlike many previous studies that assume axisymmetry or ignore rotation, this work incorporates realistic spin rates and demonstrates their measurable effects on exit velocity, ricochet angle, kinetic-energy loss, and lateral deviation.
2. **Systematic multi-parameter investigation**

This research integrates the combined influence of impact velocity, rotation, L/D ratio, nose shape, and target thickness—parameters that are rarely studied together. The findings reveal nonlinear interactions that cannot be captured through simplified analytical models.

3. **High-fidelity validation using experimental data**
   The LS-DYNA model is validated against the well-known experiments of Børvik et al. [22], achieving 5–10% accuracy in exit velocities, which is significantly better than many existing numerical ricochet studies.
4. **Practical relevance to armor and projectile design**
   By quantifying how rotation alters critical ricochet angle, energy dissipation, and trajectory deviation, this study provides actionable insights for optimizing armor thickness, composite layering, and projectile geometry in military protection applications.

In summary, this research addresses a recognized but largely unresolved challenge in the literature: the accurate numerical prediction of ricochet considering projectile spin. The proposed modeling approach improves upon existing analytical and numerical frameworks by capturing asymmetric deformation, torque-induced deviation, and energy dissipation mechanisms that traditional axisymmetric models cannot represent.

2. Methods

2.1. Research Description

This study numerically investigates the ricochet behavior of the 7.62 mm APM2 armor-piercing projectile during oblique impacts on AA6082-T4 aluminum targets. The projectile features a hardened steel core with a brass jacket and is designed for armored target penetration. The primary aim is to provide a detailed analysis of ricochet phenomena, taking into account the projectile's axial rotation, which is often neglected in simulations due to computational complexity.

Key parameters considered include impact velocities ranging from 830 to 1800 m/s, target thicknesses of 10, 20, and 30 mm, various projectile nose shapes (flat, hemispherical, ogival), and different length-to-diameter ratios (L/D). Simulation scenarios examine both cases with axial rotation (clockwise and proportional to linear velocity) and without rotation.

The main objective is to determine the critical ricochet angle (θ_c), at which the projectile fails to penetrate the target and instead ricochets. This angle depends on several factors, including the initial impact angle, velocity, and material properties. For validation, the results are compared with experimental data from Borvik et al. [22], which includes impact tests of APM2 projectiles on aluminum plates at various angles.

Additionally, this study investigates the effects of parametric factors such as trajectory deviation, energy loss, and deformation of both the projectile and the target.

2.2. Numerical Framework

To simulate this complex phenomenon, LS-DYNA software is employed. It is an advanced hydrodynamic code capable of analyzing dynamic problems at high strain rates [23]. LS-DYNA is widely used in ballistic engineering due to its robust ability to model material behavior under extreme loading, such as penetration and ricochet. The simulation workflow consists of three main stages: pre-processing, numerical solution, and post-processing.

During pre-processing, the geometry of both projectile and target is modeled with high precision to accurately capture key features, including nose shape and target thickness. Finite element meshing is performed, with a finer mesh in the impact region to improve computational accuracy.

The numerical solution can be carried out using several dynamic methods, including Lagrangian, Eulerian, ALE[1], SPH[2], and boundary element approaches [25]. In this study, the Lagrangian method is chosen due to its suitability for tracking deformation and displacement of solid materials [26]. It effectively models the interaction between the projectile and target, which involves large deformations and potential failure.

Other methods have specific applications: the Eulerian method is suitable for material flow, such as melting or dispersion, but is less relevant here since the focus is on solid deformation. The ALE method, combining Lagrangian and Eulerian features, provides flexibility for complex problems. SPH is effective for simulating extensive failure and material dispersion, while boundary elements are mainly used for surface and boundary analysis [25].

Material behavior is modeled using the modified Johnson-Cook model, which accounts for plasticity and its dependence on strain rate and temperature [27].

$$\sigma^{pl} = [A + B(\varepsilon^{pl})^n]\left[1 + \left(\frac{\dot{\varepsilon}^{pl}}{\dot{\varepsilon}_0}\right)\right]^C \left[1 - \hat{\theta}^m\right] \quad \textbf{(3)}$$

In the Johnson-Cook model, A represents the initial yield stress, B the hardening parameter, n the hardening exponent, C the strain rate sensitivity, m the temperature dependency exponent, ε the plastic strain, $\dot{\varepsilon}$ the normalized strain rate relative to a reference rate, and $\hat{\theta}$ the homologous temperature (defined as the ratio of the current temperature to the melting temperature). This model provides high accuracy for metallic materials under dynamic loading and effectively simulates the behavior of both aluminum and steel.

For predicting material failure, the Cockcroft-Latham criterion is applied [28].

$$W = \int_0^{\epsilon_{eq}} < \sigma_1 > d\epsilon_{eq} \leq W_{cr} \quad \textbf{(4)}$$

In the Cockcroft-Latham criterion, σ_1 is the maximum principal stress, and ϵ_{eq} is the strain at failure. This criterion is well-suited for ductile materials such as aluminum and steel, as it considers a combination of stress and strain.

LS-DYNA was initially developed in the 1970s by the Livermore Software Technology Corporation and has since become a standard tool for ballistic simulations [23]. The software has undergone frequent updates, including version R7.0 in 2013, and its parallel computing capabilities allow efficient use of advanced hardware to reduce computation time. Despite these advantages, challenges remain in terms of precise parameter calibration and validation of simulation results.

[1] Adaptive Lagrangian-Eulerian

[2] Smoothed Particle Hydrodynamics

2.3. Modeling

In this study, modeling involves the precise definition of geometry, materials, and boundary conditions for the projectile and target. The APM2 projectile was modeled using three-dimensional finite elements.

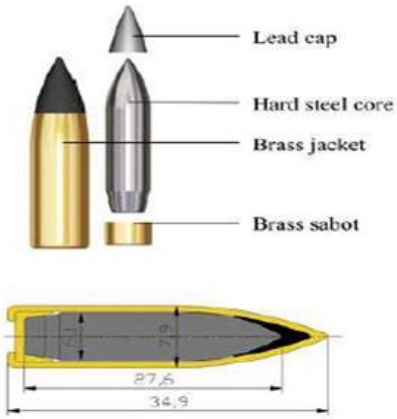

Figure 3. Geometry and dimensions of the AMP2 projectile

The projectile model consists of two main components: a steel core, which is primarily responsible for penetration, and a brass jacket that protects the core and influences its interaction with the target. Meshing of the projectile is performed with particular attention to critical regions, such as the tip and edges, to accurately capture deformation and failure mechanisms. The thickness of the jacket and its mechanical properties—including elastic modulus and yield strength—are precisely implemented in the model. The target is modeled as a plate made of AA6082-T4 aluminum alloy.

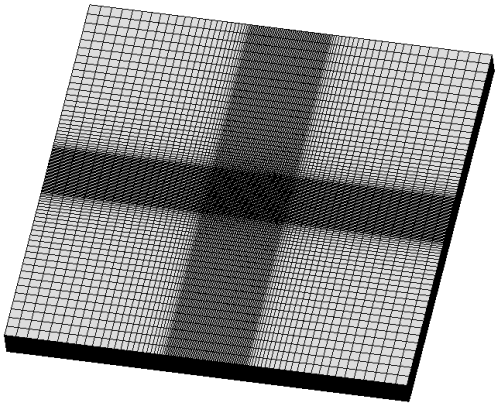

Figure 4. The meshed target with dimensions of 300*300*20 mm

This material was selected because of its ductility and widespread use in lightweight armor applications. The target mesh is refined in the impact zone, with element sizes of approximately 0.5 mm, while coarser elements are used in regions farther from the impact. This strategy balances computational efficiency with accuracy and is especially important for simulations involving high strain rates, which generate stress waves and localized deformations.

Material constants for the Johnson-Cook model and the Cockcroft-Latham criterion were obtained from reliable sources [27–31]. For AA6082-T4 aluminum, the reported values are: A≈240 MPa, B≈400 MPa, n≈0.42, C≈0.01 and m≈1.0 [29]. For the steel core of the projectile, higher values (A≈500 MPa) were used to reflect its greater strength.

Table 1. Specifications of the APM2 Projectile

Weight (g)	Max Diameter (mm)	Length (mm)	Projectile Components / Specifications
4.4	7.9	34.9	Jacket (brass CuZn10)
4.0	6.2	4	Cap (brass CuZn10)
5	6.1	27.6	Core (hardened steel)
0.7	5.1	9.3	Filler cap (lead)

Boundary conditions include fixing the edges of the target and applying an initial velocity to the projectile. The impact angle (θ) is varied parametrically to determine the critical ricochet angle (θ_c). For cases with rotation, the angular velocity is applied according to the Greenhill formula and is proportional to the linear velocity.

The simulation procedure involves defining contact between the projectile and target using LS-DYNA's automatic contact algorithm, applying dynamic loading, and recording outputs such as exit velocity, kinetic energy, and deformation patterns. Model validation was performed by assessing the effect of reducing target size (***Figure 5***) to ensure that smaller dimensions do not affect the results. Mesh sensitivity was also investigated by comparing results for different mesh sizes (***Figure 6***). Comparison with experimental data from Borvik et al. [22] (***Table 2***) shows that exit velocities and deformation patterns agree within 5–10% error, confirming the accuracy of the simulation model.

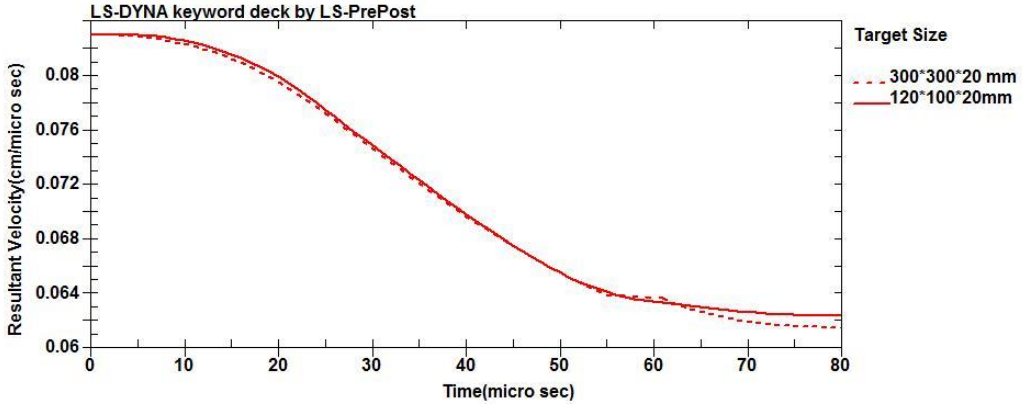

Figure 5. Output velocity of projectile from two targets with respect to target size (impact velocity equal to 830 m/s and spin rate of 0.02 radians per microsecond)

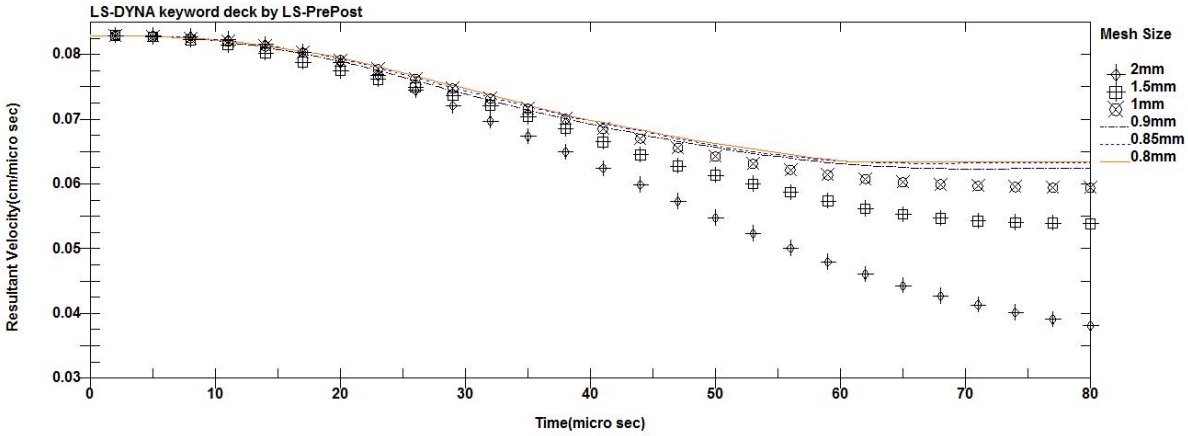

Figure 6. Output velocity of projectile from target versus different mesh sizes

Table 2. Comparison of Numerical Simulation in LS-DYNA with Experimental Work and Simulation by Borvik and Colleagues

Angle β	Bullet Exit Velocity from Target (m/s) [22]	Bullet Exit Velocity from Target with IMPETUS Simulator (m/s) [22]	Simulated Bullet Exit Velocity from Target Considering Axial Rotation (m/s)	Simulated Bullet Exit Velocity from Target Without Considering Axial Rotation (m/s)
0°	720	698	728	690
15°	719	698	725	687
30°	708	675	699	662
45°	592	551	634	543
60°	Bullet gets stuck in the target	Bullet gets stuck in the target	Matches	Matches
Average Error Percentage		3.57% (negative)	2.56% (positive)	4.68% (negative)

3. Results and Discussion

3.1. Effect of Projectile Velocity on Ricochet

The critical ricochet angle (θ_c) decreases nonlinearly with increasing projectile velocity in the range of 830 to 1800 m/s for a target with a thickness of 20 mm. For the non-spinning case, the values of θ_c were recorded as 67° at 830 m/s, 74° at 1200 m/s, 77° at 1500 m/s, and 80° at 1800 m/s. This reduction is due to the increase in the projectile's kinetic energy, which allows it to penetrate at lower angles, resulting in ricochet occurring at lower critical angles. Axial rotation of the projectile has a minimal effect on θ_c (difference less than 1 degree), but it significantly impacts the exit velocity and residual kinetic energy of the projectile after ricochet, with the exit velocity in the spinning case reduced by 5 to 15 percent. This velocity reduction is attributed to energy loss due to friction and the conversion of part of the kinetic energy into heat and deformation. At higher velocities, the projectile experiences less deformation or damage, indicating higher resistance of the steel core to severe strains. Axial rotation also causes a slight

deviation to the right (up to 2 mm at 1800 m/s), which is due to the torque effects resulting from rotation and asymmetric interaction with the target surface.

Table 3. Results of APM2 Projectile Impact on a 20 mm Aluminum Target with an Impact Velocity of 600 m/s

Angle of Impact β (degrees)	Result	Description
Projectile Impact Without Applying Axial Rotation		
0	Per	The projectile exits the back of the target at a velocity of 440 m/s.
60	Ric	The bullet ricochets off the target surface at a velocity of 334 m/s.
55	Pen	The bullet travels in a straight path along the target surface and stops within the target.
57	Ric	The bullet ricochets off the target surface at a velocity of 220 m/s.
56	Ric	The bullet stops at the moment of exiting the target surface and ricocheting.
Projectile Impact With Applying Axial Rotation (with an axial rotation speed of 0.014 radians per microsecond)		
0	Per	The projectile exits the back of the target at a velocity of 448 m/s.
55	Pen	The bullet travels in a straight path along the target surface and stops within the target.
56	Ric	The bullet ricochets off the target surface at a velocity of 28 m/s.

As shown in ***Figure 7***, the projectile impacts the target at 600 m/s and a critical angle of 56°, penetrates, changes direction, and ricochets outward. This figure compares cases with and without axial rotation to highlight the differences. The damage zone is 5 mm longer in the non-rotating case, while the maximum depth is 1 cm in both scenarios. The top view indicates that, with clockwise rotation, the core exhibits minimal deviation after ricocheting.

Figure 8 presents the velocity-time graph for this impact. In the non-rotating case, the velocity drops to zero, whereas with axial rotation, it stabilizes at 28 m/s. The stress comparison shows maximum values of 5.03 GPa for the rotating case and 4.93 GPa for the non-rotating case, both occurring at the tip of the core.

The results of the APM2 projectile impact at a velocity of 830 m/s on the target are presented in ***Table 4***. The results indicate that the projectile, in both cases with and without axial rotation, ricochets from the target surface at a critical angle of 62 degrees but with different velocities.

Table 4. Results of APM2 Projectile Impact on a 20 mm Aluminum Target, Impact Velocity of 830 m/s

Impact Angle β (degrees)	Result	Description
Projectile impact without axial rotation		
0	Per	The projectile exits the back of the target with a velocity of 690 m/s.
65	Ric	The projectile ricochets off the target surface with a velocity of 488 m/s.
63	Ric	The projectile ricochets off the target surface with a velocity of 373 m/s.
60	Pen	Part of the casing ricochets, but the core is trapped inside the target and stops.
61	Pen	The projectile is stopped inside the target.
62	Ric	The projectile ricochets off the target surface with a velocity of 189 m/s.
Projectile impact with axial rotation (axial rotation rate of 0.021 radians per microsecond)		
0	Per	The projectile exits the back of the target with a velocity of 728 m/s.
62	Ric	The projectile ricochets off the target surface with a velocity of 305 m/s.
61	Pen	The projectile is trapped inside the target.

In the graphs of ***Figure 10***, the critical angles for different impact velocities are plotted. As evident from this figure, considering or neglecting the axial rotation of the projectile has little effect on the critical ricochet angle, and only at velocities above 1800 m/s does the critical angle increase by one degree.

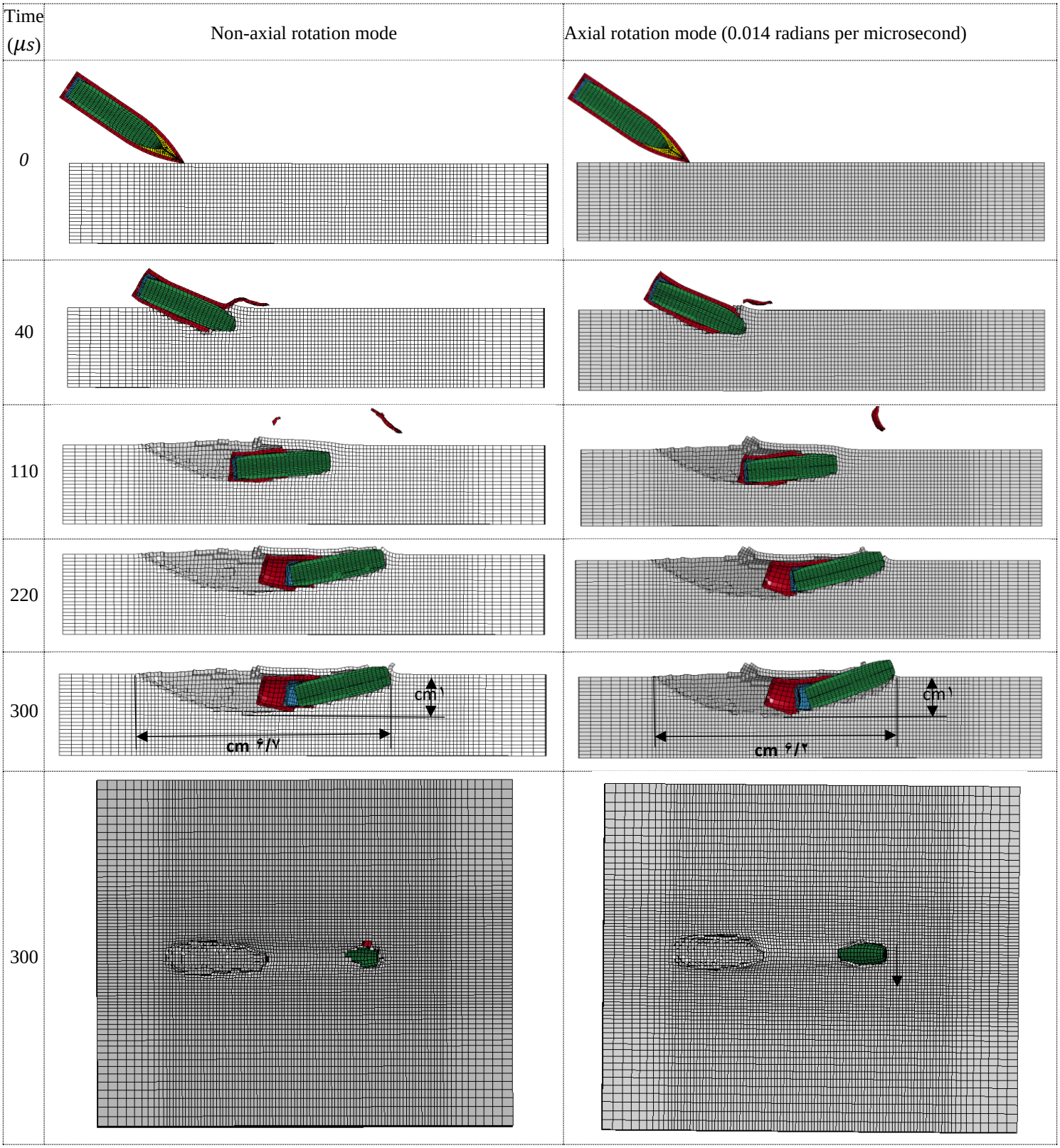

Figure 7. Impact of the projectile with a velocity of 600 m/s on a 20 mm aluminum target at an angle β = 56 degrees.

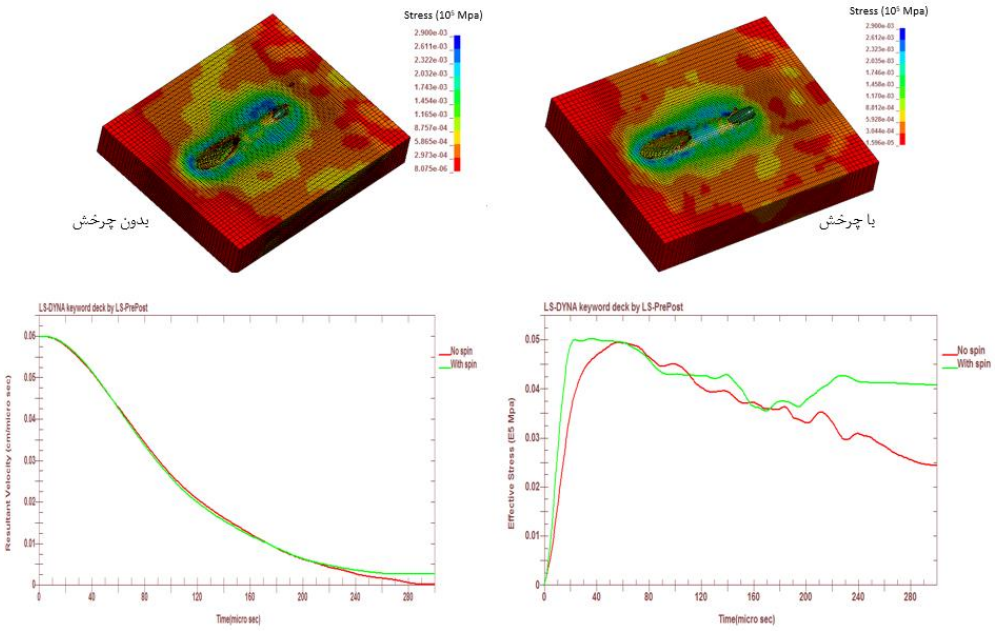

Figure 8. Stress distribution and time history of velocity and stress under an impact velocity of 600 m/s at an angle of 56 degrees.

Table 5. Results of APM2 Projectile Impact on a 20 mm Aluminum Target with an Impact Velocity of 1200 m/s

Impact Angle β (degree)	Result	Description
Projectile impact without applying axial rotation		
0	Per	The projectile exits the back of the target with a velocity of 1100 m/s.
70	Ric	The bullet ricochets off the target surface with a velocity of 535 m/s.
65	Per	The bullet exits the back of the target with a velocity of 250 m/s.
67	Ric	The bullet ricochets off the target surface with a velocity of 217 m/s.
66	Pen	The bullet causes damage to the back surface of the target and stops almost perpendicularly within the target.
Projectile impact with applied axial rotation (with an axial rotation speed of 0.023 radian per microsecond)		
0	Per	The projectile exits the back of the target with a velocity of 1110 m/s.
67	Ric	The bullet ricochets off the target surface with a velocity of 320 m/s.
66	Pen	The bullet causes damage to the back surface of the target and stops almost perpendicularly within the target.

Table 6. Results of APM2 Bullet Impact on an Aluminum Target with an Impact Velocity of 1800 m/s

Impact Angle β (degree)	Result	Description
Projectile impact without applying axial rotation		
0	Per	The projectile perforates the target with a velocity of 1700 m/s.
70	Per	The bullet exits the back of the target with a velocity of 870 m/s.
75	Ric	The bullet ricochets off the target surface with a velocity of 278 m/s.
73	Per	The bullet exits the back of the target with a velocity of 183 m/s.
74	Ric	The bullet, despite damaging the back of the target, ricochets with a velocity of 41 m/s.
Projectile impact with applied axial rotation (with an axial rotation speed of 0.034 radian per microsecond)		
0	Per	The projectile exits the back of the target with a velocity of 1710 m/s.
75	Ric	The bullet ricochets off the target surface with a velocity of 314 m/s.
74	Per	The bullet exits the back of the target with a velocity of 448 m/s.

Table 7. Results of Projectile Exit Velocity from the Target for Various Impact Velocities of the Bullet with the Target

Impact Velocity (m/s)	Impact Angle (β)	Residual Velocity (m/s) - Without Axial Rotation	Residual Velocity (m/s) - With Axial Rotation
600	0	440	448
	55	0	0
	56	0	28
	57	220	---
	60	334	---
830	0	690	728
	60	0	---
	61	0	0
	62	189	305
	63	373	---
	65	448	---
1200	0	1100	1110
	65	250	---
	66	0	0
	67	217	320
	70	535	---
1800	0	1700	1710
	70	870	---
	73	183	---
	74	41	448
	75	278	314

The residual velocity results for impacts at various velocities are presented in ***Table 7***. Note that for each impact, the velocity corresponding to the critical ricochet angle is highlighted in dark color.

According to the graph in ***Figure 11a***, the exit velocity for a projectile with a linear velocity of 1200 m/s and an angular velocity of 0.023 radians per microsecond is 103 m/s higher than that of a projectile with only linear velocity. This occurs despite the fact that, as shown in the graph in ***Figure 11b***, at the moment of impact initiation, the kinetic energy from the projectile's rotation accounts for only 0.25% of the total kinetic energy of the projectile.

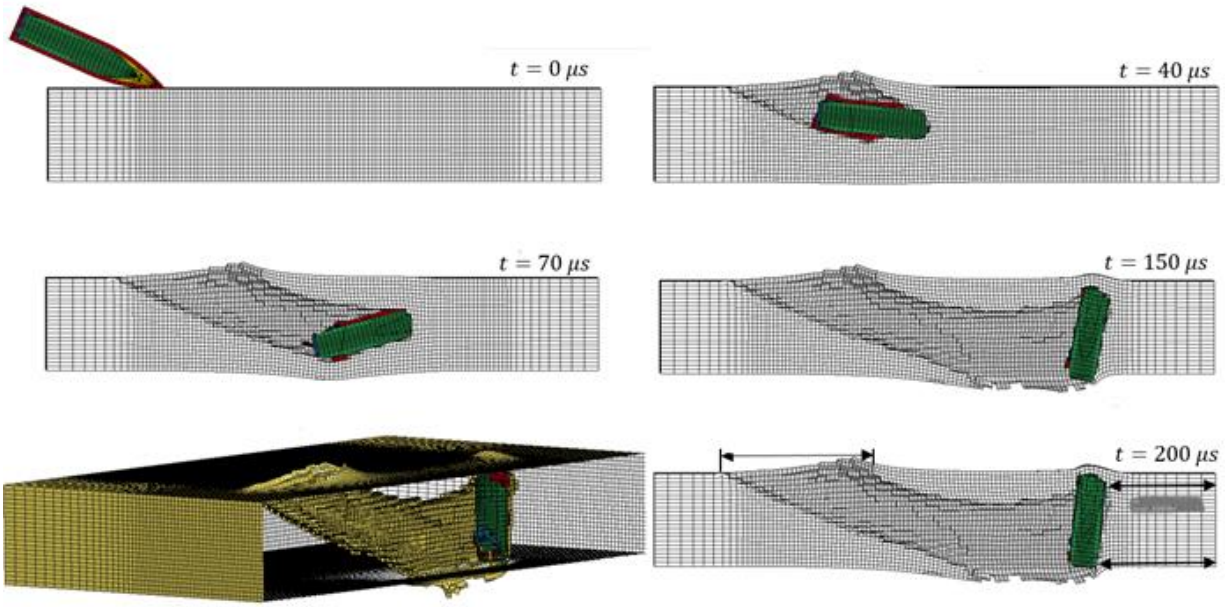

A

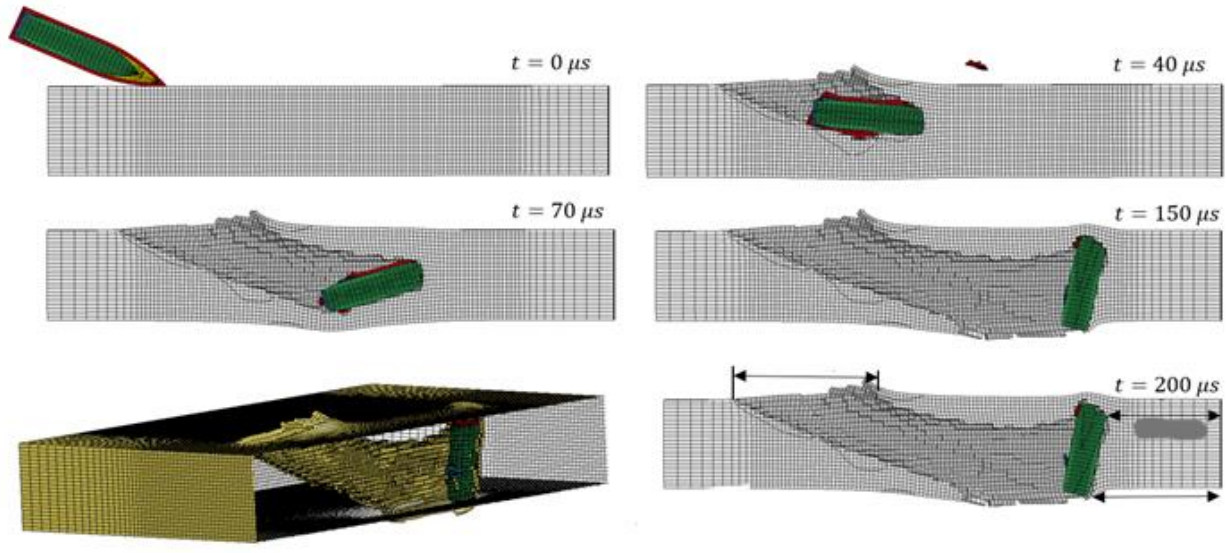

B

Figure 9. Impact of a projectile at 1200 m/s on a target at $\beta = 66$, A: Without Axial Spin, B: With Axial Spin

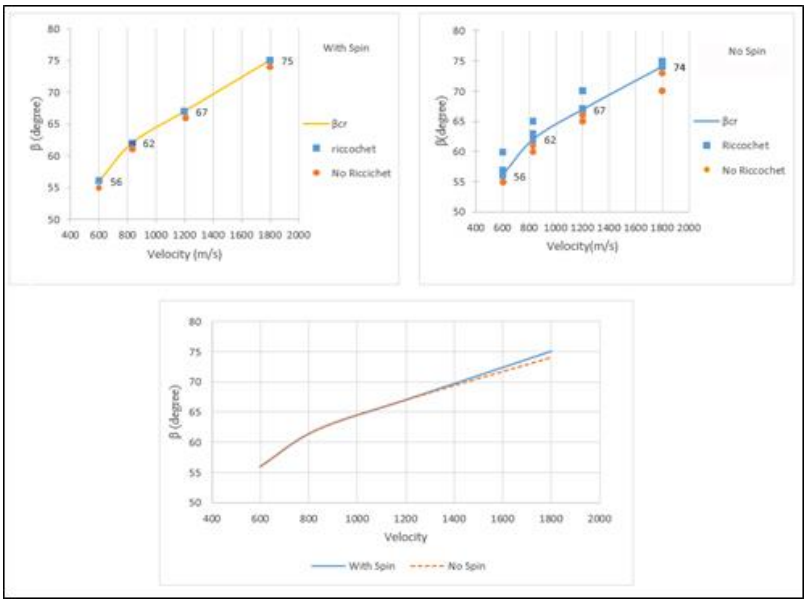

Figure 10. Critical Rebound Angle versus Impact Speed for Different Impact Velocities

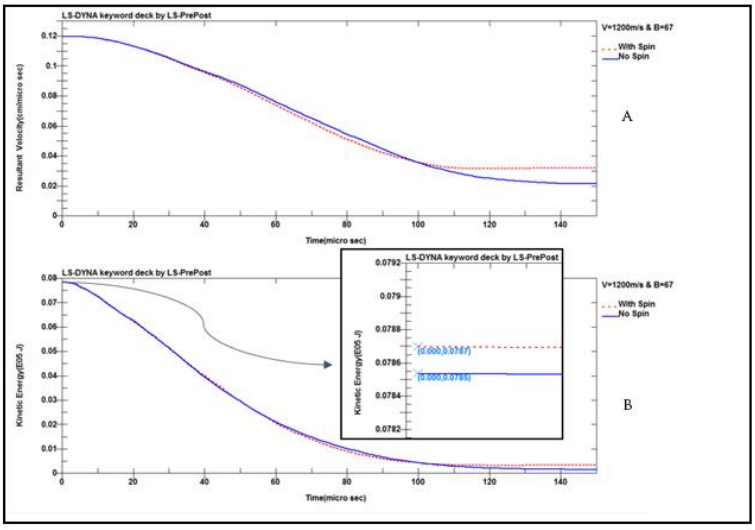

Figure 11. (A) Velocity-time graph; (B) Kinetic energy-time graph for a projectile with a linear velocity of 1200 m/s in two cases: with and without axial rotation.

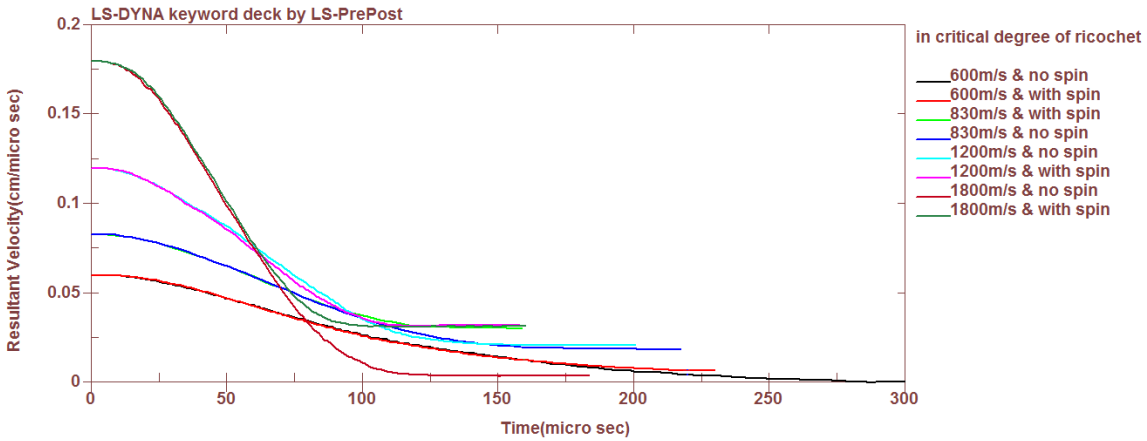

Figure 12. Velocity-time graph of the projectile impact on the target at critical angles.

3.2. Effect of Target Thickness on Ricochet

Increasing the target thickness from 10 mm to 30 mm leads to a reduction in the critical ricochet angle (θ_c), as greater thickness enhances the mechanical resistance of the target and extends the penetration path. For an impact velocity of 1200 m/s, $\theta_c$was measured as 74° for a 10 mm thickness, 67° for 20 mm, and 65° for 30 mm. This reduction indicates that with increasing thickness, the projectile ricochets at smaller angles, as its energy is consumed in attempting full penetration. Axial rotation has no significant effect on θ_c but reduces the exit velocity of the projectile. The internal energy of the target increases with greater thickness and oblique angles, as a portion of the projectile's kinetic energy is converted into plastic deformation and heat in the target. In the case with rotation, energy dissipation is higher due to additional friction between the projectile and the target and rotational effects. These findings suggest that target thickness plays a pivotal role in determining the ricochet pattern, and rotation can amplify dynamic effects.

Table 8. Results of APM2 Bullet Impact at Different Velocities on Aluminum Targets with Varying Thicknesses

Impact Velocity 1200 (m/s)													
Target Thickness (mm)		30				20				10			
Impact Angle (β)		70	66	65	64	70	67	66	65	75	74	73	70
Residual Velocity (m/s)	Without Axial Rotation	604	325	218	0	535	217	0	250	689	514	152	880
	With Axial Rotation	--	---	255	0	--	320	0	---	---	518	165	---
Impact Velocity 830 (m/s)													
Target Thickness (mm)		30				20				10			
Impact Angle (β)		62	61	60		65	63	62	61	60	73	67	66	65
Residual Velocity (m/s)	Without Axial Rotation	324	207	0		488	373	189	0	0	693	296	230	520
	With Axial Rotation	---	214	0		---	---	305	0	---	---	310		---

In ***Figure 13***, the graph of the critical ricochet angle of the projectile from targets with thicknesses of 10, 20, and 30 mm is shown for impact velocities of 1200 m/s and 830 m/s, and for two cases: with and without rotation. It is observed that as the target thickness increases, the critical ricochet angle decreases. With further increases in target thickness, the slope of the graph decreases.

3.3. Effect of Projectile Nose Shape on Ricochet

The shape of the projectile's nose significantly affects the critical ricochet angle. A projectile with an ogival nose ricochets at θ_c= 57° (without rotation) and 58° (with rotation), while a flat nose ricochets at 59° (without rotation) and 60° (with rotation), and a hemispherical nose at 64° (in both cases). This trend (ogival < flat < hemispherical) is due to differences in pressure distribution at the contact point; sharper noses (like ogival) generate higher localized pressure and ricochet earlier, whereas rounder noses (hemispherical) penetrate deeper before ricocheting. The hemispherical nose, due to its larger contact area, distributes energy over a greater depth. Axial

rotation has a minor effect on θ_c, primarily related to projectile stability, particularly in sharper noses where it improves dynamic balance.

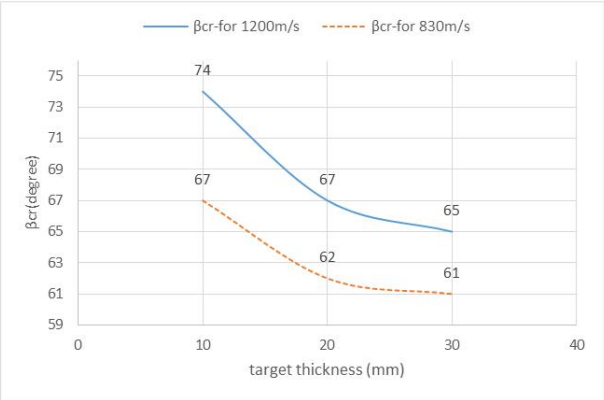

Figure 13. Effect of target thickness on the ricochet phenomenon of the projectile from the target.

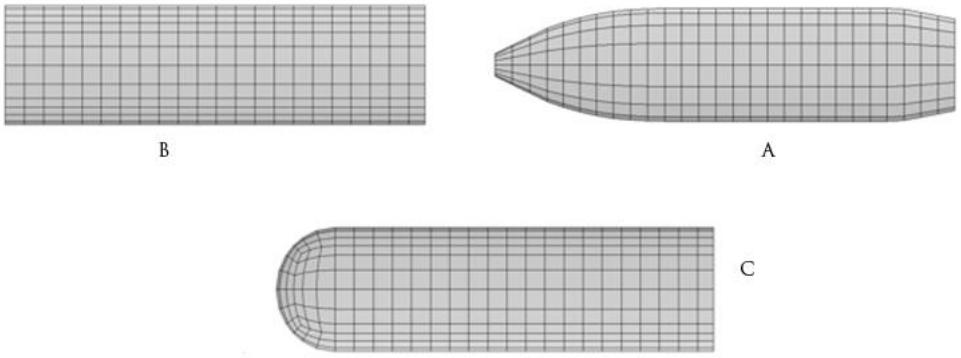

Figure 14. Geometry of projectiles with an approximate weight of 1.5 gr: A: Ogival projectile, B: Flat-nosed projectile, C: Hemispherical-nosed projectile

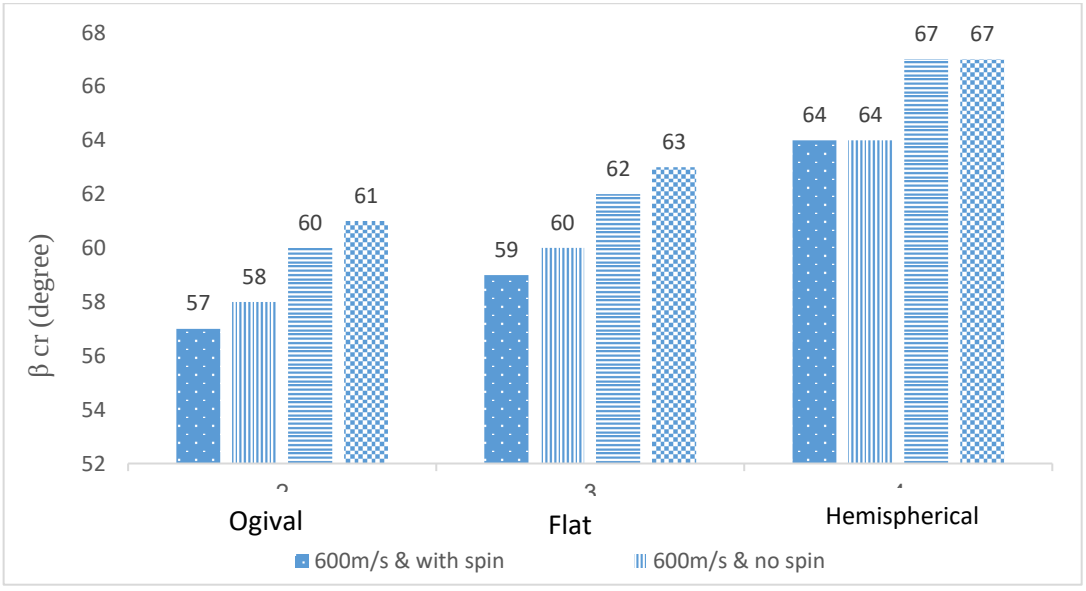

Figure 15. Critical Angle of Three Projectile Shapes under Different Velocities and Two Conditions (With and Without Axial Rotation)

3.4. Effect of Length-to-Diameter Ratio on Ricochet

Increasing the length-to-diameter ratio (L/D) leads to a non-linear increase in the critical ricochet angle, as longer projectiles exhibit lower resistance to penetration and distribute their energy over a longer path. This effect is attributed to reduced structural stiffness and increased flexibility of the projectile with higher L/D ratios. Penetration resistance decreases as L/D increases. Axial rotation amplifies these effects, as the additional torque from rotation can influence projectile stability and increase energy dissipation. Projectiles with higher L/D ratios ricochet at more oblique angles, which is significant for the design of projectiles with varying aspect ratios.

In this section, the impact of a cylindrical projectile with a hemispherical nose, weighing approximately 1.5 grams, and with aspect ratios of 1.80, 2.59, 3.71, and 6.07, was simulated on a 20 mm aluminum target at an impact velocity of 830 m/s, in two conditions: with and without axial rotation.

Table 9. Comparison of Output (Residual) Velocity of Ogival and Flat-Nosed Projectiles for Cases with and without Axial Rotation

Impact Velocity 600 (m/s)														
Geometry of the Projectile Head		Hemispherical				Flat					Ogival			
Impact Angle (β)		65	64	63	60	63	61	60	59	58	60	58	57	56
Residual Velocity (m/s)	Without Axial Rotation	187	86	0	0	169	153	--	27	0	--	158	127	0
	With Axial Rotation	224	146	0	0	194	--	71	0	--	--	162	0	0
Impact Velocity 830 (m/s)														
Geometry of the Projectile Head		Hemispherical				Flat					Ogival			
Impact Angle (β)		68	67	66	65	63	62	61	60		61		60	59
Residual Velocity (m/s)	Without Axial Rotation	258	124	0	0	205	163	0	0		-		39	0
	With Axial Rotation	-	135	0	-	134	0	-	-		236		0	-

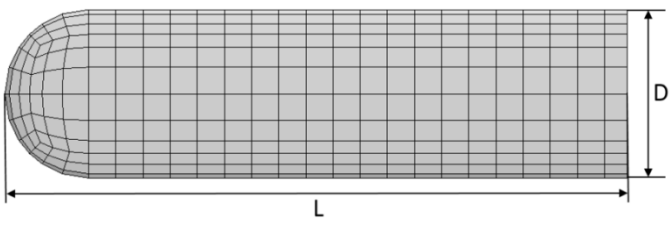

Figure 16. Geometric shape of the hemispherical-nosed projectile.

Table 10. Specifications of the cylindrical hemispherical-nosed projectile with different aspect ratios.

Projectile Number	L (cm)	D (cm)	Aspect Ratio (L/D)
1	1.438	0.8	1.80
2	1.818	0.7	2.59
3	2.291	0.617	3.71
4	3.165	0.52	6.07

Table 11. Rotational speed of the hemispherical-nosed projectile with various aspect ratios.

Projectile Number	Angular Velocity (rad/μs)
1	0.008
2	0.012
3	0.026
4	0.041

The impact results of projectile number 1 are presented in ***Table 12***. The results indicate that this projectile ricocheted at an angle of 61 degrees in both cases.

Table 12. Results of the impact of hemispherical projectile No. 1 with a velocity of 830 meters per second on a target with a thickness of 20 millimeters

Impact Angle β (degree)	Result	Description
Projectile impact without applying axial rotation		
60	Pen	The projectile stops at the verge of ricocheting from the target surface.
61	Ric	The projectile ricochets from the target surface at a speed of 80 meters per second.
Projectile impact with applying axial rotation		
61	Ric	The projectile ricochets from the target surface at a speed of 104 meters per second.
60	Pen	The projectile gets stuck inside the target.

Results of the impact of projectile No. 2 are presented in ***Table 13***. The results indicate that this projectile, at a critical angle of 64 degrees, ricocheted from the target surface in both cases, with a speed increase of 10 meters per second for the case with projectile rotation.

Table 13. Results of the impact of hemispherical projectile No. 2 at a velocity of 830 m/s on a target with a thickness of 20 mm

Impact Angle β (degree)	Result	Description
Projectile impact without axial spin		
67	Ric	The projectile ricochets off the target surface at a velocity of 341 m/s.
66	Ric	The projectile ricochets off the target surface at a velocity of 266 m/s.
64	Ric	The projectile ricochets off the target surface at a velocity of 168 m/s.
62	Pen	The projectile stops inside the target.
63	Pen	The projectile comes to rest inside the target.
Projectile impact with axial spin		
64	Ric	The projectile ricochets off the target at a velocity of 178 m/s.
63	Pen	The projectile embeds/stops inside the target.

The impact results of projectile number 3 are presented in ***Table 14***. The results indicate that this projectile ricocheted at a critical angle of 67 degrees in both cases. The exit velocity at this angle for the non-rotating and rotating cases is 124 m/s and 135 m/s, respectively.

Table 14. Results of the impact of hemispherical projectile No. 3 with a velocity of 830 meters per second on a target with a thickness of 20 millimeters

Impact Angle β (degree)	Result	Description
Projectile impact without applying axial rotation		
65	Pen	The projectile gets stuck inside the target.
68	Ric	The projectile ricochets from the target surface at a speed of 258 meters per second.
67	Ric	The projectile ricochets from the target surface at a speed of 124 meters per second.
66	Pen	The projectile gets stuck inside the target.
Projectile impact with applying axial rotation		
67	Ric	The projectile ricochets from the target surface at a speed of 135 meters per second.
66	Pen	The projectile gets stuck inside the target.

The impact results of projectile number 4 are presented in ***Table 15***. The results indicate that this projectile ricocheted at a critical angle of 69 degrees in both cases. The exit velocity at this angle for the non-rotating and rotating cases is 150 m/s and 154 m/s, respectively.

Table 15. Results of the impact of hemispherical projectile No. 4 with a velocity of 830 meters per second on a target with a thickness of 20 millimeters

Impact Angle β (degree)	Result	Description
Projectile impact without applying axial rotation		
70	Ric	The projectile ricochets from the target surface at a speed of 281 meters per second.
67	Pen	The projectile gets stuck inside the target.
68	Pen	The projectile gets stuck inside the target.
69	Ric	The projectile ricochets from the target surface at a speed of 150 meters per second.
Projectile impact with applying axial rotation		
69	Ric	The projectile ricochets from the target surface at a speed of 154 meters per second.
68	Pen	The projectile gets stuck inside the target.

Table 16 summarizes the impact results for cylindrical projectiles with hemispherical noses and various aspect ratios. The results show that axial rotation does not affect the critical ricochet angle. However, increasing the projectile's aspect ratio leads to a higher critical ricochet angle. Additionally, the percentage difference in exit velocities decreases as the aspect ratio increases.

Table 16. Results of Oblique Impact of a Hemispherical-Nosed Projectile with Different Aspect Ratios on a 20 mm Target

Projectile Aspect Ratio		1.80		2.59					3.71				6.07			
Impact Angle (β)		60	61	62	63	64	66	67	65	66	67	68	67	68	69	70
Remaining Velocity (m/s)	Without Axial Spin	0	80	0	0	168	266	341	0	0	124	258	0	0	150	281
	With Axial Spin	0	104	-	0	178	-	-	-	0	135	-	-	0	154	-

In the graph of ***Figure 17***, the critical ricochet angle for the hemispherical-nosed projectile with different aspect ratios is plotted.

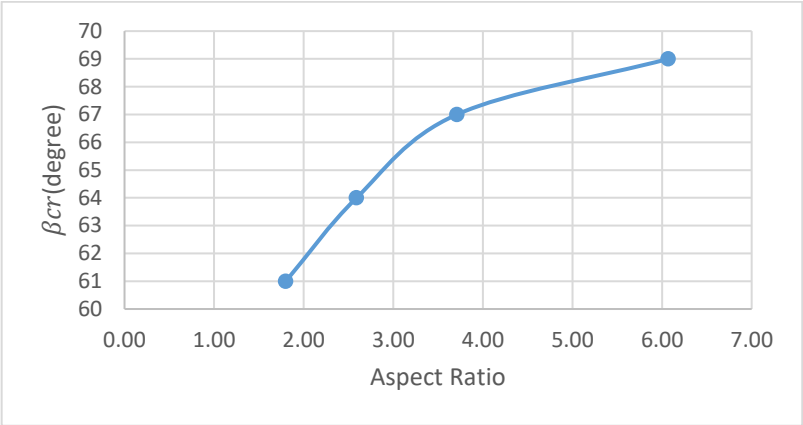

Figure 17. Results of the critical ricochet angle of the projectile with respect to different projectile aspect ratios (the result holds true for both cases with and without axial rotation).

4. Conclusion

This numerical study using LS-DYNA provides deep insights into the ricochet behavior of the APM2 projectile on AA6082-T4 targets, emphasizing the importance of considering axial rotation. Validation with experimental data from Borvik et al. [22] demonstrates that the model achieves high accuracy (5-10% error in exit velocities). Parametric results indicate that projectile velocity has an inverse effect on θ_c; increasing the velocity from 830 to 1800 m/s raises the critical ricochet angle from 67° to 80°, as the interaction time with the target decreases, making penetration at smaller angles less likely. Axial rotation, while having a minor effect on θ_c (<1°), reduces exit velocity by up to 15% and significantly lowers kinetic energy, attributed to energy dissipation through friction and rotational effects [21, 22]. A rightward deviation (up to 2 mm at 1800 m/s) caused by rotational torque is critical for predicting post-ricochet trajectories [19-20].

Target thickness reduces θ_c from 74° (10 mm) to 65° (30 mm) at 1200 m/s by increasing the resistive path, and rotation significantly enhances internal energy absorption. These findings align with classical models such as Tate [12] and Johnson [14], highlighting the pivotal role of thickness in target resistance. The projectile nose shape creates distinct ricochet patterns; ogival noses ricochet at θ_c= 57°, flat noses at 59°, and hemispherical noses at 64°, related to pressure distribution and deeper penetration of rounder noses [32, 33]. Rotation slightly increases θ_c for sharper noses, contributing to dynamic stability.

The length-to-diameter ratio (L/D) non-linearly increases θ_c, reducing penetration, as longer projectiles are more flexible and exhibit lower resistance. Rotation amplifies these effects by increasing torque and energy dissipation, consistent with long rod theories [34, 35]. Neglecting rotation leads to an incomplete representation of energy dynamics and invalidates symmetry assumptions [21], as it significantly affects post-ricochet behavior. It is recommended that field experiments with simulated conditions, the use of composite targets, advanced damage models (e.g., Johnson-Cook damage [27]), and other software (e.g., Autodyn [25]) or methods like SPH be employed for further validation. These findings enhance the optimization of armor and projectile design [1, 16, 22].

References

[1] Backman, M. E., & Goldsmith, W. (1978). The mechanics of penetration of projectiles into targets. *International Journal of Engineering Science*, *16*(1), 1-99.

[2] Jonas, G. H., & Zukas, J. A. (1978). Mechanics of penetration: analysis and experiment. *International Journal of Engineering Science*, *16*(11), 879-903.

[3] Badurowicz, P., & Pacek, D. (2022). Determining ricocheting projectiles' temperature using numerical and experimental approaches. *Materials*, *15*(3), 928.

[4] Wu, Y., Tao, X., & Xue, Y. (2022). Analytical investigation of ricochet range of ogive—shaped nose projectile obliquely penetrating thick steel target. *Applied Sciences*, *12*(9), 4692.

[5] Lang, Z. H. A. N. G., Fengpeng, Z. H. A. O., Yuzhong, Z. H. A. N. G., Yongjun, D. E. N. G., & Jicheng, L. I. (2025). Ballistic performance of tungsten fiber-reinforced metallic glass composite in the long rod oblique penetration/perforation. *Explosion And Shock Waves*, *45*(3), 033302-1.

[6] Eren, M. I., Romans, J., Walker, R. S., Buchanan, B., & Key, A. (2024). Bullet ricochet mark plan-view morphology in concrete: an experimental assessment of five bullet types and two distances using machine learning. *Forensic sciences research*, *9*(1), owad051.

[7] Paige, J., Walker, R. S., Buchanan, B., Key, A., Romans, J., & Eren, M. I. (2025). Elliptical Fourier analysis of bullet ricochet impact site plan-view shape in concrete. *Forensic Sciences Research*, *10*(3), owaf010.

[8] Xu, X., Wu, Y., Jia, Y., & Gan, S. (2024). Analysis of the Inclined Impact Resistance Characteristics of Concrete Structures Against Projectiles. In *International Conference on Civil Engineering* (pp. 744-753). Singapore: Springer Nature Singapore.

[9] Hosseinkia, & Mahdipour Omrani, A. (2012). *Fundamentals of ballistics* (in Persian). Malek Ashtar University of Technology.

[10] Wikipedia. (Accessed via historical data). http://en.wikipedia.org

[11] Adapted from dissertation images; original source not specified.

[12] Tate, A. (1979). A simple estimate of the minimum target obliquity required for the ricochet of a high-speed long rod projectile. *Journal of Physics D: Applied Physics*, *12*(11), 1825–1829.

[13] Reid, S. R., Edmonds, A. J., & Johnson, W. (1981). Bending of long steel and aluminum rods during end impact with a rigid target. *Archive: Journal of Mechanical Engineering Science*, *23*(2), 85–92.

[14] Johnson, W., Sengupta, A. K., & Ghosh, S. K. (1982). Plasticine modeling of the high-velocity oblique impact and ricochet of long rods. *International Journal of Mechanical Sciences*, *24*(7), 437–455.

[15] Johnson, W., et al. (1983). Modelling with plasticine the low speed impact of long rods against inclined rigid targets. *International Journal of Impact Engineering*, *1*(1), 73–83.

[16] Goldsmith, W. (1999). Non-ideal projectile impact on targets. *International Journal of Impact Engineering*, *22*(2-3), 95–395.

[17] Børvik, T., et al. (2002). Perforation of 12 mm thick steel plates by 20 mm diameter projectiles with flat, hemispherical, and conical noses. *International Journal of Impact Engineering*, *27*(1), 19–35.

[18] Rosenberg, Z., et al. (2005). Ricochet of 0.3-inch AP projectile from inclined polymeric plates. *International Journal of Impact Engineering*, *31*(3), 221–233.

[19] Segletes, S. B. (2006). A model for rod ricochet. *International Journal of Impact Engineering*, *32*(9), 1403–1439.

[20] Segletes, S. B. (2007). Further development of a model for rod ricochet. *International Journal of Impact Engineering*, *34*(5), 899–925.

[21] Rosenberg, Z., Ashuach, Y., & Dekel, E. (2007). More on the ricochet of eroding long rods—validation of an analytical model with 3D simulations. *International Journal of Impact Engineering*, *34*(5), 942–957.

[22] Børvik, T., et al. (2011). Normal and oblique impact of small arms bullets on AA6082-T4 aluminum protective plates. *International Journal of Impact Engineering*, *38*(7), 577–589.

[23] Livermore Software Technology Corporation. (2013). *LS-DYNA keyword user's manual: Volume I* (Version R7.0).

[24] Altair Engineering Company. (2001). Basic HyperMesh Altair Hyperworks 5.0 tutorial.

[25] Darian, A. S., & Jalali, S. (n.d.). *Impact and explosion engineering with a comprehensive guide to AUTODYN software* (in Persian). Darian Engineers Publications.
[26] Sheikh Kousar, A. A., & Delayli, H. (2007). Analysis of deformation of circular steel plates under underwater explosion using finite element software (LS-DYNA) and comparison with experimental results (in Persian) [Report]. Faculty of Marine Engineering, Malek Ashtar University of Technology.
[27] Børvik, T., Hopperstad, O. S., Berstad, T., & Langseth, M. (2001). A computational model of viscoplasticity and ductile damage for impact and penetration. *European Journal of Mechanics-A/Solids*, *20*(5), 685–712.
[28] Cockcroft, M. G., & Latham, D. J. (1968). Ductility and workability of metals. *Journal of the Institute of Metals*, *96*, 33–39.
[29] Dey, S. (2004). *High-strength steel plates under projectile impact: An experimental and numerical study* (Doctoral dissertation). Department of Structural Engineering, Norwegian University of Science and Technology, Norway. ISBN 978-82-471-6282-8.
[30] Dey, S., Børvik, T., Hopperstad, O. S., & Langseth, M. (2006). On the influence of fracture criterion in projectile impact of steel plates. *Computational Materials Science*, *38*(1), 176–191.
[31] Børvik, T., Dey, S., & Clausen, A. H. (2009). Perforation resistance of five high-strength steel plates subjected to small arms projectiles. *International Journal of Impact Engineering*, *36*(7), 948–964.
[32] Murali, V., Low, M. G., & Naik, S. D. (2012). Study of critical ricochet angle for conical nose shape projectiles. *AIP Conference Proceedings*, *1482*, 58–63.
[33] Hazell, P. J., et al. (2013). The effect of gilding jacket material on the penetration mechanics of a 7.62 mm armour-piercing projectile. *International Journal of Impact Engineering*, *54*, 11–18.
[34] Daneshjou, K., & Shahravi, M. (2008). Penetrator strength effect in long-rod critical ricochet angle. *Journal of Mechanical Science and Technology*, *22*(11), 2076–2089.
[35] Daneshjou, K., Shahravi, M., & Babaei, B. (2009). *Ricochet of long rod steel projectiles from deformable steel plates* [Paper presentation]. 17th Annual (International) Conference on Mechanical Engineering-ISME.